Muscle Actuator Design for the ACT Hand

Nick Gialias[*] and Yoky Matsuoka[†,§]
[*]Biomedical Engineering, [†]Robotics Institute, [§]Mechanical Engineering
Carnegie Mellon University
Pittsburgh, PA USA

Abstract - **We are constructing an anatomically-correct testbed (ACT) of the human hand to understand its mechanisms, function, and neural control. As a part of this effort, we created an actuator that mimics both the active and passive behaviors of the human muscles. To use it as the actuator of the ACT Hand, it must conserve the tendon-driven structure so that the size or the weight of the hand do not have to be compromised. A custom-made spring composite was used to simulate the human's nonlinear passive muscle stiffness closely ($R^2 = 0.99$). A coreless DC motor was used to siumulate the active contraction. The passive and active components interacted in parallel and they were attached to a cable tendon that inserted into the bones. In order to study the neural control of hand movements, we incorporated Hill's model in the active contraction component. Therefore, the computer program could simply specify the muscle activation level, and the appropriate tendon tension could be provided given the current muscle length. This muscle actuator allowed an accurate realization of neural activation based control of ACT Hand, and it provides a foundation for intimate brain-machine interface.**

Keywords - artificial muscles; robotic hand; anatomically correct testbed; anthropomorphic; brain-machine interface

I. INTRODUCTION

Amongst the most challenging problems in present day robotics is to integrate biological and robotic systems. Two intriguing and coupled problems are the development of a human-like robotic hand and a brain-machine interface with that device. This is a new field of research in robotics and many fundamental issues in this field are yet to be solved. For example, the control inputs related to the human brain signal are being explored [1, 2]. Furthermore, there are several robotic limbs capable of using these inputs and performing in a fairly natural way 3, 4], but they are often constrained to their limitations such as the limited degrees of freedom. In order to understand the neural control of fine manipulation skills and to provide these skills to people without them, it is important to create a robotic hand that preserves most of the human's anatomy.

In order to create such a device, we initiated development of an anatomically correct testbed (ACT) Hand [5, 6]. This hand, unlike many anthropomorphic robotic hands, incorporates biomechanical aspects of the anatomy that are functionally crucial in order to use control signals that resemble the neural commands. For example, the tendon insertion points (where the tendons attach to the bones) and the routing of the tendons including the extensor mechanism are preserved [5]. Bones have been constructed that conserve the complex human geometry [6]. This geometry has been found to play an essential role in proper tendon routing and therefore conserves the natural tension vectors necessary for human-like execution of movement. Joints have been developed that conserve the range of motion and theoretical joint stiffness' have been estimated [6]. To be able to control these biomechanically accurate components, this anatomical robotic hand must also have muscle-like actuators that incorporate human muscle properties. As a first step towards an entire hand, we are currently developing a complete index finger, which has all associated muscles.

Many actuators have been developed to simulate muscles. Some of these include: shape memory alloys [7], hydrogel polymers [8] and pneumatics [9]. The most popular muscle-like actuators in practice are McKibben style pneumatic actuators because it is small and compliant [10, 11]. In addition, it responds quickly unlike hydrogel polymers and has a reasonable travel length compared to shape memory alloys. However, upon closer inspection of natural muscle properties, it becomes evident that the compliance of the McKibben muscle is significantly different from to the compliance of the real muscles.

Alternatively, a system that utilizes servomotors could provide more precise muscle-like properties through control. For our ACT Hand, it is currently more crucial to mimic the active and passive behavioral properties than to be completely self-contained, thus the use of servomotors fits our needs. Rather than modeling and providing all passive behavior through active motor drive, a nonlinear custom-made spring can be added in parallel to the servomotor. This parallel structure provides faster response, necessary compliance for stable force control [12, 13], and simpler control algorithm for the motor drive.

In this paper, we describe an actuator that mimics both the active and passive behaviors of the human muscles using a servomotor and a custom-made spring. We first review human muscle properties (Section II), describe the model, design, and development of the passive spring (Section III), and the integration of the active and passive components to complete the entire actuator (Section IV). In order to study the neural control of hand movements, we incorporated Hill's model in the active contraction component (Section V). Therefore, the computer program could simply specify the muscle activation level (rather than current, voltage, position, or force), and the appropriate tendon tension could be provided given the current muscle length. Finally Section VI combines active and passive components to establish the total length-tension characteristic.
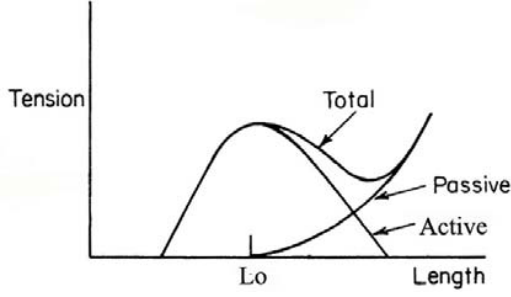
Fig. 1 Isometric length-tension curve for human parallel-fibered skeletal muscle from [14]. The figure shows three curves: Active, Passive and Total, where total is equal to the sum of active and passive.

TABLE 1
INDEX FINGER MUSCLES

Muscle	Lo (in)	Tmax (lbs)
Extensor Indicis	2.2	5.4
Extensor Digitorum Communis	2.2	5.4
Flexor Digitorum Profundus	2.6	14.59
Flexor Digitorum Superficialis	2.8	10.81
Palmer Interosseous 1	0.6	7.03
Dorsal Interosseous 1	1	17.3
Lumbrical	2.2	1.08

II. HUMAN MUSCLE PROPERTIES

Skeletal muscles control human movement.   This biological actuator produces tension through the overlap and interaction of thin and thick protein filaments called actin and myosin, respectively [15]. The nature of this interaction causes the muscle to contract and thereby produce a unidirectional tension. Fig. 1 shows a typical isometric length-tension curve for human skeletal muscle.   The passive curve is a nonlinear spring property of muscle when stretched beyond resting length (*Lo*). The parabolic active curve is due to the overlap of actin and myosin filaments. The amount of overlap of thick and thin filaments and therefore tension is a function of the muscles length. The active tension, *Ta,* could be described by

$$Ta = \alpha \left\{ \frac{-T_{max}(dx)^2}{Lo^2} + T_{max} \right\} \quad (1)$$

where α is a scaling variable that corresponds to neural activation normalized from 0 (no activation) to 1 (maximum activation), T_{max} is maximum active tension and dx is the change in muscle length measured from *Lo*.   Constants T_{max} and *Lo* for all the index finger muscles are listed in Table 1 (calculated from [16]).   The passive tension, *Tp,* could be described by

$$Tp = \frac{T_{max}(e^{ksh*dx/dx_{max}} - 1)}{e^{ksh} - 1}, \quad L \geq L_0 \quad (2)'$$

where k_{sh} is a shape parameter between 1 and 4 and depends on the property of the muscle and dx_{max} is the maximum length change of the muscle typically taken to be 0.5 *Lo*. Finally the total tension is described to be the sum of active and passive tensions,

$$T_{total} = Ta + Tp . \quad (3)$$

In order to execute movements, the human central nervous system must take the length-tension property into account in order to efficiently supply the proper activation to muscles. An efficient controller should account for the inhibition of movement by an antagonist muscle's passive tension when stretched beyond *Lo*. The muscle activation level, α, in (1) is the control input, which can be used to scale the size of the active parabolic curve shown in Fig. 1 and therefore modulates the muscle's length-tension relationship.

The human musculotendon system has two forms of feedback, which detect tension and positional information. The position is encoded from a sensory structure called the muscle spindle. The muscle spindle is capable of detecting both static position information as well as dynamic information of the muscle. The second form of sensory information is encoded by a structure called the Golgi tendon organ. The Golgi tendon organ detects the amount of tension in the muscle by having a collagen helical structure with embedded nerves. When the structure is stretched the nerve is compressed by the collagen and tension information is relayed.

In the following sections, we describe how we simulated these biological properties for the ACT Hand.

III. A MODEL OF PASSIVE MUSCLE PROPERTY

The passive property of the isometric muscle characteristic is modeled using (2). This equation indicates that tension in the muscle increases exponentially with an increase in length. In addition to its role in muscle tension production, the passive component also gives instantaneous compliance to the joints. This helps to stabilize the joints when contact is made with an object or when perturbed by an outside force.

In order to mimic the biological passive property, we used a silicon tube and a polyethylene terephthalate mesh. These individual materials are similar to those used for McKibben actuators.   However, unlike the pneumatic actuator this structure is only used as a passive element for our actuator design.   Therefore, the length-tension characteristic of the composite is completely independent of the active component. The polyethylene terephthalate mesh encapsulating the silicon tube creates a nonlinear length-tension relationship similar in nature to human muscle. By changing the diameter, wall thickness, and length of the silicon tube the length-tension relationship can be changed. The nonlinear stiffness can be tuned by changing the density of the mesh or by changing the entire length of the composite.

To match the typical eccentricity of (2) for a human index finger muscle, we first determined a mesh density to be 30x0.010" filaments per 0.125" ID and silicon tube size to be 5/32x7/32". A number of tube and mesh combinations were tested. This particular combination was chosen because it

Fig. 2 Synthetic passive tension composite material. The composite is constructed from a silicon tube and polyethylene terephthalate mesh, fixed to hose barbs with cyanoacrylate and bound with wire ties. This specific composite shown is 2.0 inches from the inner surfaces of the hose barbs
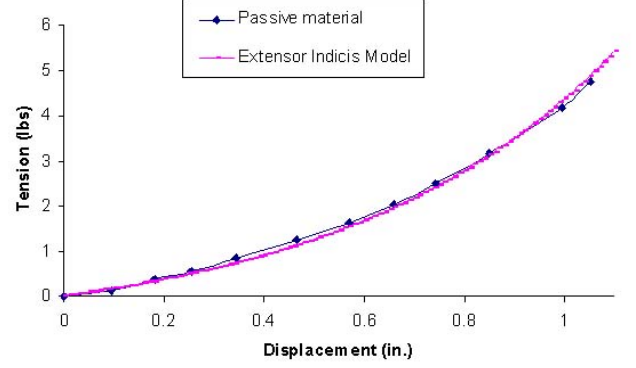

Fig. 3 Isometric length-tension curves for passive composite (Length = 6.5 inches) & the extensor indicis (EI) muscle model. The material is initially at zero tension and zero displacement and then is displaced by 1.1 inches. R^2 = 0.99.

TABLE 2

COMPOSITE LENGTHS

Muscle	Composite Lc (in)
Extensor Indicis	6.5
Extensor Digitorum Communis	6.5
Flexor Digitorum Profundus	3.5
Flexor Digitorum Superficialis	5.4
Palmer Interosseous 1	1.9
Dorsal Interosseous 1	2.2

closely matches the eccentricity of human hand muscles and reaches the necessary tension value within the size constraint of our system. These values allowed six of the seven index finger muscles to be constructed by changing the total lengths of both materials. Both ends of the composite were fixed to brass hose barbs, glued with a cyanoacrylate, and bound with wire ties. The assembled passive muscle component is shown in Fig. 2.

To model the relationship between the composite length and the passive spring length-tension function, we conducted a tensile testing with seven composites with different lengths (1, 2, 3, 4, 5, 6, and 7 inches). The tensile testing was performed on a Sintech system 1 device using Testworks v3.10 software. Each of the seven composites was displaced by .25 in/min to a maximum tension of 15 pounds. Using these results, we modeled the relationship between the composite length, Lc, passive spring tension, $Tpc,$ and displacement, dx to be

$$Tpc = \frac{a(e^{bc*dx} - 1)}{e^b - 1} \qquad (4)$$

$$a = a_0 + a_1 Lc + a_2 Lc^2 + a_3 Lc^3 + a_4 Lc^4 \qquad (5)$$

$$b = b_0 + b_1 Lc \qquad (6)$$

$$c = c_0 + c_1 Lc + c_2 Lc^2 + c_3 Lc^3 + c_4 Lc^4 \qquad (7)$$

where the coefficients a and c are 4th order polynomial functions of the composite length, and b is a linear function of the composite length that varies between 1 and 4 similarly to k_{sh} .

Additional nearly linear stiffness was added when the passive spring was connected to the ACT Hand through the cables, attachments and routing fixtures. This elasticity was accounted for when determining the necessary composite length. Table 2 shows the composite lengths for the index finger muscles. The lumbrical is excluded due to its extremely low tension / length ratio. For this muscle, a small linear spring is used.

The first muscle chosen to mimic was the extensor indicis, an extrinsic muscle of the hand. It has a relatively low tension / length ratio and therefore is one of the longest composites. The extensor indicis' resting length is 2.2 inches and reaches a tension of 5.4 pounds when displaced by 1.1 to a length of 3.3 inches [17]. Fig. 3 compares length-tension curves for the extensor indicis passive tension model in (2) with k_{sh} =2 and our passive nonlinear composite. The displacement is measured from the resting length of the material, and our passive composite curve closely the muscle model (R^2 = 0.99).

IV. A MODEL OF ACTIVE MUSCLE PROPERTY AND INTEGRATION OF MUSCLE ACTUATOR

Our muscle actuator was a combination of the passive spring composite described above and the active contraction that was supplied by a MicroMo 2342 24CR coreless DC motor with a 43:1 planetary gearbox. The total tension, $Ttotal$, was produced by the passive spring tension, Tpc in (4) and the active contraction tension, Ta produced as shown in Fig. 4. Motor control software was written in Visual C++, which interfaces with a DSP series motion controller (Model PCX/DSP, Motion Engineering, Inc. Santa Barbara, CA). A motor amplifier (model TA105, Trust Automation, San Luis Obispo, CA) was used in current mode to supply the motor input.

We incorporated two forms of feedback sensors in the active component of the muscle actuator. To mimic the muscle spindles (muscle length sensitive sensors), we incorporated optical encoders that accurately record the position of the motor rotation. To mimic the Golgi tendon organs (muscle tension sensitive sensors), we designed a strain gage cantilever beam that was attached between the motor shaft and a pulley that spooled the tendon cable. A 1.5-inch OD pulley with bearing rotated freely around the motor shaft so that all the force exerted onto the tendon cable was conducted on the cantilever. The tendon cable was then attached to the pulley and routed using sheaves. By tracking the motor rotation and the tension on the strain gage, the length of the passive component could also be deterministically identified.
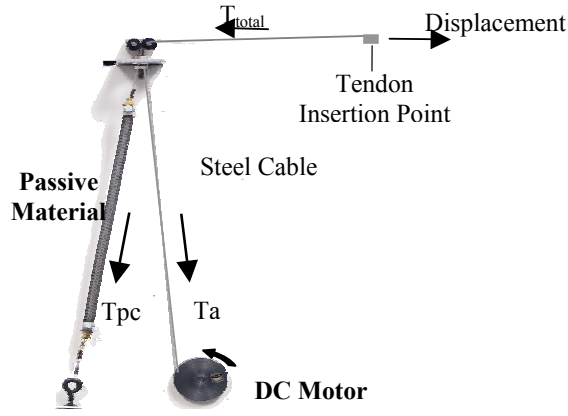
Fig.4 Picture of the active component (DC Motor) and passive component (composite material) placed in parallel. The passive component only produces tension when displaced beyond the resting length and the active component only produces tension in one direction. The two components attach at the tendon insertion point and sum to produce $T_{total} = Tpc + Ta$.
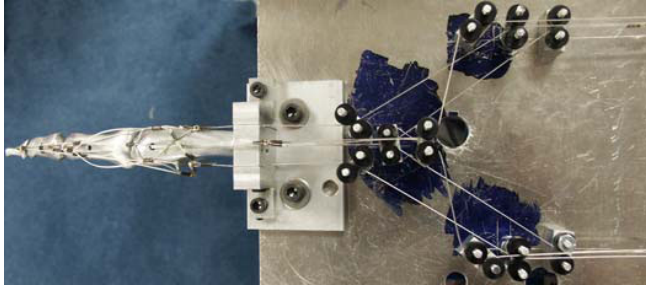

Fig. 5 Our ACT index finger apparatus. The finger has 4 bones, 4 degrees of freedom, an extensor hood, 7 muscles, which are routed with delrin sheave fixtures. Each tenson insertion has two connections, one for the active contraction and another for passive tension.

The tension sensor was placed near the motors rather than right on the hand for two reasons. First, lightweight cables were used to transmit tension; therefore a sensor placed in series would weigh down the cable and add additional unwanted tension. Second, 54 cables will eventually be routed to the hand (one for active tension and one for passive tension for each of the 27 hand muscles) and series sensors placed near the hand would become tangled with one another.

To run the passive and active components in parallel, Delrin sheaves (0.38 inch OD) are used to route the cable from the motor and the passive composite to their insertion points on the bones as shown in Fig. 5, which are placed in the physiological position. The sheaves are positioned such that the muscle tension vectors are conserved. According to (1) and (2), Tp should only be engaged at values of $L \geq Lo$ so that the passive property is left with slack when the muscle is shorter than the rest length. If the material were placed in series with the cable then Tp would become a function of Ta, which does not follow (2).
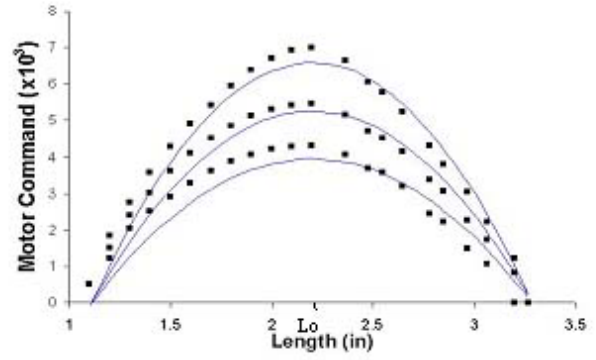

Fig. 6 Motor command vs. length for the extensor indicis muscle actuator. The curves correspond to α values from 0.6, 0.8 and 1.0. The square points correspond to values of motor command data and the solid line is from (9). R^2 were 0.91, 0.95, and 0.97 respectively. These data are used to determine the necessary motor command to generate a length-tension curve.

V. INTEGRATED MUSCLE ACTUATOR RESPONSE WITH HILL'S MODEL

In order to study the neural control of movement using this ACT Hand, we incorporated Hill's model (Fig.1). This means that each integrated muscle actuator takes a normalized muscle activation level $(0<\alpha<1)$ rather than the motor or muscle torques, and outputs appropriate muscle tension. In order to map the relationship between the command that should be sent to the motor and the muscle activation level, α, we first mapped the relationship between the motor command, MC, and the active tension, Ta, recorded at the bone insertion point of the actuator while the passive composite was disconnected. This relationship can be approximated as

$$Ta = C_1 MC + C_2 \qquad 8)$$

where $C_1 = 0.8$ (10^3 lbs/MC) and $C_2 = 0.1315$ (lbs). Using (8) and (1), we determined the relationship for generating a motor command by supplying a level of activation, α to be

$$MC = \frac{\alpha\left\{\dfrac{-T_{max}(dx)^2}{Lo^2} + T_{max}\right\} - C_2}{C_1}. \qquad (9)$$

Using this relationship between the motor command and the muscle activation level, the muscle's length-tension property was determined by holding a constant activation value. Fig. 6 shows a series of those curves for $\alpha = 0.6$, 0.8, and 1.0. The curve shown is the theoretical value calculated using (9), and the curve and the data matched closely, $R^2 > 0.90$.

Once the relationship between the muscle activation and the motor commands was established for the muscle actuator, we connected the passive composite material in parallel to
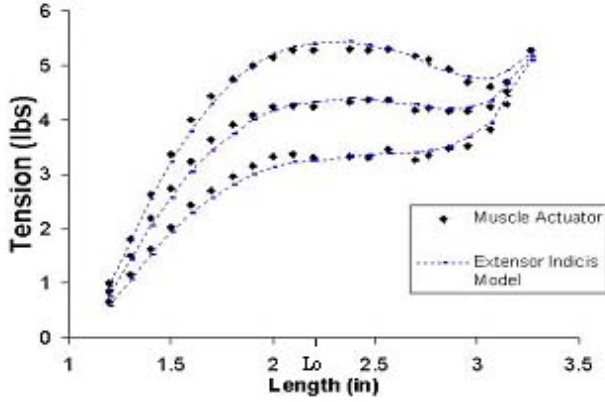
Fig. 7 Isometric length-tension curve. The square points correspond to the data collected and the dashed line corresponds to the passive tension model for the extensor indicis. The curves correspond to α values from 0.6, 0.8 and 1.0. R^2 was = 0.99.

record the total length-tension curve. We set the parallel structure so that the passive material's rest length (where the passive material had no slack but experienced no tension) was at 2.2 inches to match the property of extensor indicis. We slowly pulled on the cable at the bone insertion point from 2.2 to 3.266 inches in roughly 0.1 inch intervals locking the force sensor in place at each interval (measurements at lengths from 1.1 to 2.2 were taken at the same position because the passive element is slack and does not affect the length-tension relationship) At each interval we input a series of α values and measured the total tension developed. Fig. 7 shows three of these length-tension curves recorded, each of them corresponding to different α (0.6, 0.8, and 1.0). The curves plotted are *Ttotal* from (3) for the extensor indicis muscle for the corresponding α values. Our length-tension curve matched closely (R^2 = .99) to the theoretical value for any given α.

VI. DISCUSSION

We have successfully incorporated the passive compliance that matches the human muscles with a custom-made composite that was incorporated in parallel with a servomotor. Unlike other muscle-like actuators, muscle's isometric length-tension property has also been incorporated through open-loop control of the motor. In order to study the neural control strategies used when people are involved in isometric tasks (such as grasping objects), it is crucial that we map the tension of each tendon to muscle activation.

In-vivo studies have been conducted to measure muscle tension by placing sensors directly on the tendon [17]. These studies have revealed crucial information to understand muscle tension during movements. However, limitations exist because of the invasive nature of this surgical procedure that don't allow for each muscle tension to be measured. Therefore, important aspects of the muscle control such as muscle synergies have not been fully analyzed. The ACT Hand using accurate muscle actuators will be able to address key issues that current in-vivo methods cannot.

Another biological fact that could be analyzed using our new actuators is the length of the muscles when the index finger is in its equilibrium. While each muscle has a rest length, this is not necessarily the length that the muscle sits when the finger is at rest because the finger reaches equilibrium when all muscle forces balance out each other, not when each muscle force is equal to 0. These lengths are difficult to measure with simple experiments because it is a redundant system and there are multiple solutions. By turning off all the motors and conducting a system identification experiment, we can validate the results with the human index finger.

We demonstrated our capability to match the extensor indicis, an extrinsic muscle of the hand, but this method can be applied to any muscles. We have already constructed six muscles that control the index finger, and verified their performance against the model. To do so, we used (4) to calculate the length of the composite material required and matched the size of the DC motor to the maximum tension of that muscle. We derived (4) assuming that we are only interested in mimicking the hand muscles. We know that if the muscle of our interest is significantly stronger or longer than the hand muscles, (4) will not be valid. When we need to make the muscles outside of the hand, we plan to use an alternative silicon tube or nylon mesh to tune the material properties.

The main drawback of using DC motors is that they have poor torque / weight ratios. In general these actuators are not suitable in applications that have strict constraints on size and weight such as wearable prosthetics. Fortunately, our system is not limited by this constraint. Another typical problem associated with DC motors is cogging and stiction, but they were greatly reduced by using coreless motors and elastic elements.

As our next step, we will incorporate a dynamic contraction model into our muscles. Hill's tension-velocity model of muscle contraction will be used as a first approach to incorporate dynamics into actuator.

[1] M.A.L. Nicolelis, "Brain-machine interfaces to restore motor function and probe neural circuits," *Nat Rev Neuroscience*, vol 4 pp. 417-422, 2003.

[2] D.M. Taylor, S.I. Tillery A.B. Schwartz, "Direct cortical control of 3D neuroprosthetic devices," *Science*, vol 296, pp. 1829-1832, 2002.

[3] R.F. Weir, D.S. Childress, "Prostheses and artificial limbs," *Encylopedia of Applied Physics*, vol. 15, pp. 115-140, 1996.

[4] K. Ito, M. Ito, etal, "Compliance control of an EMG-controlled prosthetic forearm using ultrasonic motors," Intelligent Robots and Systems, Advanced Robotic Systems and the Real World, IROS. Proc. IEEE/RSJ/GI International Conference on, vol. 3 pp. 12-16, vol. 3, pp. 1816-1823, 1994.

[5] D. D. Wilkinson, M. V. Weghe, Y. Matsuoka, "An extensor mechanism for an anatomical robotic hand," *Proc. IEEE International Conf. on Robotics and Automation*, vol. 1, pp. 238-243, 2003.

[6] M. Vande Weghe, M. Rogers, M. Weissert, Y. Matsuoka, "The ACT Hand: Design of the Skeletal Structure," *in press, IEEE International Conf. on Robotics and Automation*, 2004.

[7] C. Pfeiffer, K. DeLaurentis, C. Mavroidis, "Shape memory alloy actuated robot prostheses: initial experiments," *IEEE International Conference on Robotics and Automation,* vol. 3 pp. 10-15, 1999.

[8] M. Suzuki, "An artificial muscle by PVA hydrogel can generate high power close to living skeletal muscles, " Engineering in Medicine and Biology Society, Images of the Twenty-First Century, Proc. Of the Annual International Conference of the IEEE Engineering in, 9-12, vol. 3 pp.916-917, 1989.

[9] D. Caldwell, G. A. Medrano-Cerda, M. Goodwin, "Characteristics and Adaptive Control of Pneumatic Muscle Actuators for a Robotic Elbow," *Proc. IEEE International Conf. on Robotics and Automation*, pp. 3558-3563, 1994.

[10] P., Carbonell, Z. P. Jiang, D.W. Repperger, "Nonlinear control of a pneumatic muscle actuator: backstepping vs. sliding-mode," *Proc. IEEE International Conf. on Control Applications*, pp. 167-172, 2001.

[11] B. Tondu, P. M. Lopez, "Modeling and control of McKibben artificial muscle robot actuators," *IEEE Control Systems Magazine*, pp. 15-38, 2000.

[12] G. A. Pratt, M. W. Williamson, "Series Elastic Actuators," *IEEE International Conference on Intelligent Robots and Systems,* vol. 1, pp. 399-406, 1995.

[13] K. Ito, M. Ito, etal, "Compliance control of an EMG-controlled prosthetic forearm using ultrasonic motors," Intelligent Robots and Systems, Advanced Robotic Systems and the Real World, IROS. Proc. IEEE/RSJ/GI International Conference on, vol. 3 pp. 12-16, , vol. 3, pp. 1816-1823, 1994.

[14] .Newman,http://paperairplane.mit.edu/16.423J/Space/SBE/muscle/musclemechanics2003.pdf

[15] A.F. Huxley, "The origin of force in skeletal muscle," *Ciba Found Symp*, vol. 31 pp. 271-290, 1975.

[16] P.W. Brand, A.M. Hollister, "Mechanics of individual muscles at individual joints," *Clinical Mechanics of the Hand*, 3rd edition, Mosby, Inc,pp. 100-183, 1999.

[17] J.T. Dennerlein, "Measuring human finger flexor muscle force in vivo: revealing exposure and function", *Skeletal Muscle Mechanics: From Mechanisms to Function,*. John Wiley & Sons, Ltd. pp. 429-451, 2000.

[18] M. Hamerlain, "An anthropomorphic robot arm driven by artificial muscles using a variable structure control," *Proc. IEEE/RSJ International Conf. on Intelligent Robots and Systems*, pp. 550-555, 2000.